

## Article

# Performance Analysis of RIS-Assisted SatComs Based on a ZFBF and Co-Phasing Scheme

Minchae Jung <sup>1</sup>, Taehyoung Kim <sup>2,\*</sup> and Hyukmin Son <sup>3,\*</sup>

<sup>1</sup> Department of Electronics and Information Engineering, Sejong University, Seoul 05006, Republic of Korea; mcjung@sejong.ac.kr

<sup>2</sup> School of Electrical Engineering, Kookmin University, Seoul 02707, Republic of Korea

<sup>3</sup> Department of Electronic Engineering, Gachon University, Seongnam 13120, Republic of Korea

\* Correspondence: th.kim@kookmin.ac.kr (T.K.); hson102@gachon.ac.kr (H.S.)

**Abstract:** In recent high-throughput satellite communication (SatCom) systems, the use of reconfigurable intelligent surfaces (RISs) has emerged as a promising solution to improve spectral efficiency and extend coverage in areas with limited terrestrial network access. However, the RIS may amplify the inter-beam interference (IBI) caused by multibeam transmission at the satellite, and multiple RISs can also cause inter-RIS interference (IRI) to terrestrial users. In this paper, the performance of the RIS-assisted SatCom system is asymptotically analyzed for both full and partial channel state information (CSI) scenarios. In particular, zero-forcing beamforming is considered as the active beamforming for data transmission, while the co-phasing scheme is considered as the passive beamforming for RIS reflection. Based on the asymptotic analyses, deterministic active and passive beamforming techniques using partial CSI are proposed that can gradually eliminate both IBI and IRI, ultimately achieving ideal performance. Simulation results validate the accuracy of asymptotic analyses and demonstrate the superiority of deterministic active and passive beamforming techniques using partial CSI. The simulation results also confirm that the proposed beamforming can achieve approximately 92.8% of the ideal performance, even though it only requires partial CSI.

**Keywords:** active and passive beamforming; co-phasing technique; full frequency reuse (FFR); reconfigurable intelligent surface (RIS); satellite communication; zero-forcing beamforming (ZFBF)

**MSC:** 94A05



**Citation:** Jung, M.; Kim, T.; Son, H. Performance Analysis of RIS-Assisted SatComs Based on ZFBF and Co-Phasing Scheme. *Mathematics* **2024**, *12*, 1257. <https://doi.org/10.3390/math12081257>

Academic Editors: Farag M. Sallabi and Mohammad Hayajneh

Received: 26 March 2024

Revised: 18 April 2024

Accepted: 19 April 2024

Published: 21 April 2024



**Copyright:** © 2024 by the authors. Licensee MDPI, Basel, Switzerland. This article is an open access article distributed under the terms and conditions of the Creative Commons Attribution (CC BY) license (<https://creativecommons.org/licenses/by/4.0/>).

## 1. Introduction

Recently, the demand for high-throughput satellite (HTS) systems has been increasing rapidly due to the growing number of Internet of Things (IoT) devices and emerging 6G applications [1–3]. However, existing satellite communication (SatCom) systems encounter limitations regarding signal attenuation and the ability to maintain a line-of-sight (LoS) communication link between the satellite and terrestrial user equipment (UE) caused by obstacles and shadowing. Recently, reconfigurable intelligent surfaces (RISs) have been proposed as a promising solution for supporting high-throughput SatCom systems [4–7]. RISs are passive reflecting surfaces that can control the phase, frequency, and amplitude of incoming radio frequency (RF) signals and reflect them to a desired destination [8–10]. Therefore, by using unmanned aerial vehicles (UAVs) equipped with RISs, it becomes possible to enhance the signal strength of satellites and expand the coverage of SatCom systems, especially in areas inaccessible due to obstacles and shadowing. Importantly, this can be achieved without consuming additional UAV battery power.

Previous studies [11–13] have focused on the challenges of employing UAVs as mobile relays in SatCom systems. The authors in [11] analyzed the performance of SatCom systems using UAVs equipped with multi-antenna arrays, operating as moving decode-and-forward relays. Another approach proposed in [12] explored blind beam-tracking techniques, where

UAVs equipped with large-scale antenna arrays acted as relays between satellites and terrestrial networks. Additionally, in [13], a relay architecture for UAVs operating between the ground and satellites was investigated. The studies in [5–7] examined the concept of RISs deployed on man-made structures, such as buildings and walls, to reflect or refract signals from satellites to the destinations. However, the assumption of UAVs as active relays consuming additional energy for signal processing, as presented in [11–13], is impractical due to the limited battery capacity of UAVs and the need for energy-efficient operation. Moreover, the deployment of RISs on the surface of ground structures, as assumed in [5–7], may not adequately complement existing SatCom systems or fully harness the potential for enhancing network capacity.

Meanwhile, to achieve high spectral efficiency and throughput in the upcoming multibeam HTS systems, full frequency reuse (FFR) is generally considered in SatCom systems [14]. This approach allows each beam to exploit all the available bandwidth, ensuring maximum resource utilization. However, the performance of FFR-based SatCom systems can be degraded by inter-beam interference (IBI) resulting from the overlapping side lobes between the multiple beam radiation patterns. In an RIS-assisted SatCom system, the FFR in the RIS–UE links may cause amplification of IBI, and multiple RISs may also result in inter-RIS interference (IRI) to terrestrial UEs. Moreover, acquiring full CSI for all RIS-related channels is challenging in practice [15]. Hence, integrating RIS into the SatCom system poses the inevitable challenge of mitigating IBI and IRI by relying on partial CSI of the desired channel. Recently, in [16], the performance of a two-layer RIS-assisted UAV communication system was analyzed. In [17], the authors jointly optimized user scheduling and phase shift in the simultaneously transmitting and reflecting (STAR)-RIS-assisted multicast SatCom systems. However, these studies did not consider the impact of IBI and IRI introduced by RIS on the performance of the considered system. In this paper, we conduct a performance analysis considering the impact of IBI and IRI, which are crucial factors in RIS-assisted SatCom systems.

To overcome the aforementioned limitations, we propose a deterministic zero-forcing beamforming (ZFBF) combined with the co-phasing technique that only requires partial CSI of the desired channel. In particular, the contributions of our work can be outlined as follows:

- First, we analyze the performance of the ZFBF combined with the co-phasing technique based on full channel state information (CSI) as the number of RIS elements increases towards infinity.
- To make the analysis more practical, we propose a novel deterministic ZFBF and co-phasing technique that only requires partial CSI while eliminating IBI and achieving near-optimal performance.
- Furthermore, we derive a closed-form expression for the asymptotic ergodic capacity of the proposed scheme.
- We then analyze the outage probability and demonstrate that the outage probability decreases as the number of RIS elements increases, thereby confirming the RIS's ability to provide reliable SatCom services in scenarios with a large number of RIS elements.

The simulation results validate the asymptotic optimality of the proposed scheme, showing that it closely approaches the ideal performance. Moreover, the outage probability exhibits a potential convergence to zero as the number of RIS elements increases, further supporting the reliability and efficiency of the proposed scheme.

Notations: Throughout the paper, boldface upper- and lower-case symbols represent matrices and vectors, respectively, and  $\mathbf{I}_N$  and  $\mathbf{1}_{M \times N}$  are, respectively, a size- $N$  identity matrix and an  $M \times N$  matrix of ones. The conjugate, transpose, inverse, and Hermitian transpose operators are  $(\cdot)^*$ ,  $(\cdot)^T$ ,  $(\cdot)^{-1}$ , and  $(\cdot)^H$ , respectively. The operator  $\text{diag}(a_1, \dots, a_n)$  is a diagonal operator that constructs a diagonal matrix from a vector  $[a_1, \dots, a_n]^T$ . The amplitude and phase of a complex number  $a$  are denoted by  $|a|$  and  $\angle a$ , respectively.  $E[\cdot]$  and  $\text{Var}[\cdot]$  denote expectation and variance operators, respectively, and  $\mathcal{O}(\cdot)$  denotes the big O notation.  $\mathcal{L}^2\mathcal{N}(\eta, \sigma^2)$  denotes a double-log-normal distribution with mean  $\eta$

and variance  $\sigma^2$ , and  $\otimes$  and  $\xrightarrow{\text{a.s.}}$ , respectively, denote the Kronecker product and almost sure convergence.

### 2. System Model

We present an RIS-assisted SatCom system composed of a multibeam satellite, a single Earth station (ES),  $K$  UEs with single antennas, and  $K$  UAVs each equipped with an RIS consisting of  $N$  reflecting elements. As illustrated in Figure 1, the UAVs operate as mobile reflectors between the satellite and the UEs. The satellite generates  $K$  spot beams with  $K$  feeds; each beam is fed by a single feed, and the satellite’s payload is considered to be transparent. The UAVs reflect the incident signals from the satellite using their RISs, and the phases of the incident wave are adjusted by  $N$  reflecting elements. It is assumed that the ES assigns one appropriate RIS to each UE, which means one RIS is allocated per UE, and a dedicated wireless control link is utilized to deliver a control signal from the ES to each RIS for the information of the reflection phase shift. In summary, the system operates as follows: (i) a satellite generating  $K$  beams receives signals from the ES and transmits signals to  $K$  UAVs. Subsequently, (ii) each UAV transmits a signal to each designated user through  $N$  reflecting elements. In this configuration, (iii) the UE receives IBI from the satellite through the RIS and simultaneously receives interference from adjacent RISs, referred to as IRI.

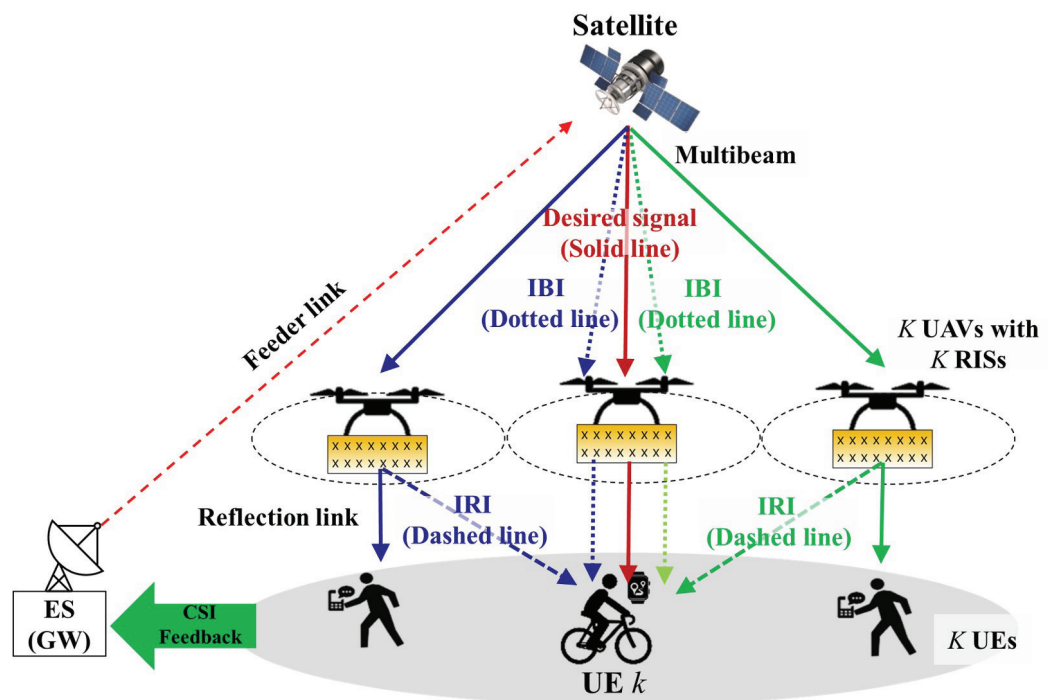


Figure 1. System model of the RIS-assisted SatCom system.

#### 2.1. RIS-Assisted SatCom Channel Model

To achieve high spectral efficiency and throughput in multibeam HTS systems, FFR is generally considered in SatCom systems [18]. However, the performance of the FFR-based SatCom system can be degraded by co-channel interference among inter-beam UAVs, particularly for UAVs at the beam edge. Consequently, the RISs installed on those UAVs reflect the incident signals, including the IBI, to the UEs. This results in severe performance degradation due to the phase-aligned and amplified IBI. Thus, in order to mitigate IBI, we assume that beamforming (i.e., active beamforming) is performed at the ES. Additionally, we consider that the feeder link is ideal, similar to most related works [5–7]. Then, the received signal at UE  $k$  is obtained as:

$$y_k = \sqrt{\rho_k} f_{k,k}^H \Phi_k D_k B_k w_k x_k + n_k$$

$$+ \sum_{i \neq k}^K \left( \underbrace{\sqrt{\rho_i} f_{k,k}^H \Phi_k D_k B_k w_i x_i}_{\text{IBI}} + \underbrace{\sqrt{\rho_i} f_{i,k}^H \Phi_i D_i B_i w_i x_i}_{\text{IRI}} \right), \tag{1}$$

where  $\rho_k$  and  $w_k \in \mathbb{C}^{K \times 1}$  are, respectively, the transmit signal-to-noise ratio (SNR) and the transmit beamforming vector for UE  $k$ , and  $f_{i,k} \in \mathbb{C}^{N \times 1}$  and  $D_k \in \mathbb{C}^{N \times N}$  are, respectively, the fading channels between RIS  $i$  and UE  $k$  and between the satellite and RIS  $k$ . Also,  $x_k$  and  $n_k$  are the transmit signal and additive complex Gaussian noise with zero mean and unit variance, respectively, and  $\Phi_k \in \mathbb{C}^{N \times N}$  is a reflection matrix that operates as a passive beamformer and can be controlled by the ES. The reflection matrix  $\Phi_k$  can be obtained as follows:

$$\Phi_k = \text{diag} \left( \sqrt{\alpha_{k,1}} e^{j\theta_{k,1}}, \sqrt{\alpha_{k,2}} e^{j\theta_{k,2}}, \dots, \sqrt{\alpha_{k,N}} e^{j\theta_{k,N}} \right), \tag{2}$$

where  $\sqrt{\alpha_{k,n}} \in [0, 1]$  and  $\theta_{k,n} \in [0, 2\pi)$  are, respectively, the amplitude and phase shifting response of the reflection element  $n$  in RIS  $k$ . Assuming lossless reflection power at all the RISs, we consider that  $\alpha_{k,n} = 1, \forall k, n$ . In (1), the signals directly transmitted from the satellite to the UEs are neglected because of severe path loss and shadowing. For a practical air-to-ground (A2G) channel,  $f_{i,k}$  is generated by a correlated Rician fading channel composed of a deterministic LoS path and a fading non-LoS (NLoS) path, as follows:

$$f_{i,k} = \bar{\beta}_{i,k} \bar{f}_{i,k} + \tilde{\beta}_{i,k} \tilde{f}_{i,k}, \tag{3}$$

where

$$\bar{\beta}_{i,k} = \sqrt{\frac{\kappa_{i,k} \zeta_{i,k}}{\kappa_{i,k} + 1}}, \tag{4}$$

$$\tilde{\beta}_{i,k} = \sqrt{\frac{\zeta_{i,k}}{\kappa_{i,k} + 1}}. \tag{5}$$

Here,  $\kappa_{i,k}$  and  $\zeta_{i,k}$  are, respectively, the Rician factor and the path loss between RIS  $i$  and UE  $k$ , and  $\bar{f}_{i,k} \in \mathbb{C}^{N \times 1}$  comprises the deterministic LoS components whose entries are determined depending on the locations of RIS  $i$  and UE  $k$ . Defining  $\bar{f}_{i,k,n}$  as the  $n$ th element of  $\bar{f}_{i,k}$ , we have  $\bar{f}_{i,k,n} = \exp(-j2\pi d_{i,k,n} / \lambda)$ , where  $d_{i,k,n}$  denotes the distance between reflecting element  $n$  of RIS  $i$  and UE  $k$ , and  $\lambda$  denotes the wavelength of a signal [19]. Also,  $\tilde{f}_{i,k} = G_i^{1/2} \hat{f}_{i,k} \in \mathbb{C}^{N \times 1}$  consists of the correlated NLoS components between RIS  $i$  and UE  $k$ , where  $G_i \in \mathbb{C}^{N \times N}$  is the spatial correlation matrix at RIS  $i$ , and  $\hat{f}_{i,k}$  is the independent NLoS component. In (1),  $D_k$  is a rain fading matrix, and  $B_k \in \mathbb{C}^{N \times K}$  is the coefficient matrix whose entries represent the gains of the beam radiation pattern with path loss between the satellite and RIS  $k$ , respectively, given as [18]:

$$D_k = |c_k| \exp(j\psi_k) I_N, \tag{6}$$

$$B_k = \sqrt{\zeta_k} a_k^T \otimes \mathbf{1}_{N \times 1}. \tag{7}$$

In (7),  $\zeta_k$  and the entries of  $a_k \in \mathbb{R}^{K \times 1}$  are the coefficients representing, respectively, the effects of the path loss and beam pattern as given by:

$$\zeta_k = \left( \frac{\lambda}{4\pi d_k} \right)^2, \tag{8}$$

$$a_{k,m} = \sqrt{G_{\max}} \left( \frac{J_1(u_{k,m})}{2u_{k,m}} + 36 \frac{J_3(u_{k,m})}{u_{k,m}^3} \right), \tag{9}$$

where  $a_{k,m}$  is the  $m$ th element of  $a_k$ ,  $d_k$  is the distance from the satellite to RIS  $k$ ,  $G_{\max}$  is the maximum gain of the satellite beam,  $J_n(\cdot)$  is the first-kind Bessel function of order  $n$ , and  $u_{k,m} = 2.07123 \frac{\sin \phi_{k,m}}{\sin \phi_{3\text{dB}}}$ . Also,  $\phi_{3\text{dB}}$  and  $\phi_{k,m}$  are the 3 dB angle of the beam and the angle

between the center of beam  $m$  and RIS  $k$ , respectively. In (6),  $|c_k|$  is the rain fading channel gain that follows a double-log-normal distribution such as  $|c_k| \sim \mathcal{L}^2\mathcal{N}(\eta_k, \sigma_k^2)$ , and  $\psi_k$  is the phase of the fading channel at RIS  $k$  that is distributed uniformly over  $[0, 2\pi)$ , as in [18]. Hence, the elements in  $\mathbf{a}_k$  and  $\mathbf{B}_k$  are deterministic values depending on the locations of the satellite and UEs.

### 2.2. ZFBF and Co-Phasing Technique

In (1), the term  $\sqrt{\rho_i} \mathbf{f}_{k,k}^H \Phi_k \mathbf{D}_k \mathbf{B}_k \mathbf{w}_i x_i$  represents IBI caused by the  $i$ th on-board feed  $\mathbf{w}_i x_i$ , while the term  $\sqrt{\rho_i} \mathbf{f}_{i,k}^H \Phi_i \mathbf{D}_i \mathbf{B}_i \mathbf{w}_i x_i$  represents IRI resulting from the  $i$ th on-board feed reflected by the  $i$ th RIS. Note that the acquisition of full CSI for RIS-related interference channels, such as  $\mathbf{f}_{i,k}$  and  $\mathbf{D}_i$ , is challenging in practice [15]. Also, ZFBF and the co-phasing technique can be designed solely based on information about the desired channels, without requiring any information about the RIS-related interference channels [18,20]. Hence, we consider ZFBF at the ES to eliminate IBI while adopting the co-phasing technique at the RIS as a suboptimal strategy to mitigate IRI.

The effective channel between the satellite and UE  $k$  via RIS  $k$  and the aggregate effective channel for  $K$  UEs are, respectively, given as:

$$\mathbf{h}_{k,k} = \mathbf{f}_{k,k}^H \Phi_k \mathbf{D}_k \mathbf{B}_k, \tag{10}$$

$$\mathbf{H} = [\mathbf{h}_{1,1}^T, \mathbf{h}_{2,2}^T, \dots, \mathbf{h}_{K,K}^T]^T. \tag{11}$$

Consider that  $\mathbf{H}$  is perfectly known at the ES. Then, the corresponding ZFBF matrix is obtained as  $\mathbf{T} = \mathbf{H}^{-1}$ . Then, the ZFBF vector for UE  $k$  can be expressed as  $\mathbf{w}_k = \mathbf{t}_k / (K \|\mathbf{t}_k\|)$ , where  $\mathbf{T} = [\mathbf{t}_1, \mathbf{t}_2, \dots, \mathbf{t}_K]$ . Here, the equal power allocation is assumed because, in high transmit power systems such as SatCom systems, the equal power allocation can achieve the performance resulting from the water-filling solution [21]. Also, to maximize the desired signal power, the phase shifts at the RIS can be designed based on the co-phasing technique such that the reflected  $N$  signals from the RIS are aligned in phase as follows:  $\theta_{k,n} = -\angle f_{k,k,n}^* \forall k, n$ , where  $f_{k,k,n}$  is the  $n$ th element of  $\mathbf{f}_{k,k}$ . Then, the received signal-to-interference-plus-noise ratio (SINR) at UE  $k$  can be obtained as follows:

$$\gamma_k = \frac{\rho_k}{K^2 \|\mathbf{t}_k\|^2 (1 + \sum_{i \neq k}^K \rho_i |\mathbf{g}_{i,k}^T \mathbf{D}_i \mathbf{B}_i \mathbf{w}_i|^2)}, \tag{12}$$

where we define

$$\mathbf{g}_{i,k} = [ |f_{i,k,1}| e^{j\theta_{i,k,1}}, |f_{i,k,2}| e^{j\theta_{i,k,2}}, \dots, |f_{i,k,N}| e^{j\theta_{i,k,N}} ]$$

and  $\theta_{i,k,n} = \angle f_{i,k,n}^* - \angle f_{i,i,n}^*$ . We can observe from (12) that the IBI is perfectly eliminated, while the IRI still remains. However, we will demonstrate that the co-phasing technique at the RIS can asymptotically mitigate the IRI as well.

### 3. Active Beamforming and Phase Shift Design

We provide an asymptotic analysis of  $\gamma_k$  in the following two scenarios: (i) full CSI is available at the ES and (ii) only partial CSI composed of the deterministic information, such as the locations of satellites and UEs, is available at the ES.

#### 3.1. ZFBF and Co-Phasing Technique Using Full CSI

Considering the ZFBF at the ES and the co-phasing technique at the RIS, the effective channel between the satellite and UE  $k$  via RIS  $k$  and the corresponding ZFBF vector for UE  $k$  can be rewritten, respectively, as follows:

$$\mathbf{h}_{k,k} = \sqrt{\xi_k} |c_k| \exp(j\psi_k) \mathbf{a}_k^T \sum_n |f_{k,k,n}|, \tag{13}$$

$$\mathbf{w}_k = \frac{\bar{\mathbf{t}}_k}{K \exp(j\psi_k) \|\bar{\mathbf{t}}_k\|}. \tag{14}$$

Here,  $\bar{\mathbf{t}}_k$  is defined as the  $k$ th column vector of  $\bar{\mathbf{T}}$ , where  $\bar{\mathbf{T}} = \bar{\mathbf{H}}^{-1}$  and  $\bar{\mathbf{H}} = [\mathbf{a}_1^T, \mathbf{a}_2^T, \dots, \mathbf{a}_K^T]^T$ . Then, the received signal at UE  $k$  can be obtained as:

$$y_k = \frac{\sqrt{\rho_k \zeta_k} |c_k| \sum_n |f_{k,k,n}|}{K \|\bar{\mathbf{t}}_k\|} x_k + \sum_{i \neq k}^K \frac{\sqrt{\rho_i \zeta_i} |c_i| \sum_n |f_{i,k,n}| e^{j\vartheta_{i,k,n}}}{K \|\bar{\mathbf{t}}_i\|} x_i + n_k, \tag{15}$$

where  $\vartheta_{i,k,n} = \angle f_{i,k,n}^* - \angle f_{i,i,n}^*$ . The second term in the right-hand side of (15) represents the residual IRI generated by the reflected signal from other RISs. As  $N$  increases, the residual IRI and the noise become negligible compared to the desired signal as follows:

$$y_k \xrightarrow[(a)]{\text{a.s.}} \frac{\sqrt{\rho_k \zeta_k} |c_k| \sum_n |f_{k,k,n}|}{K \|\bar{\mathbf{t}}_k\|} x_k. \tag{16}$$

In (16), (a) results from the following two observations: (i) as  $N$  increases,  $\sum_n |f_{k,k,n}|$  increases with  $\mathcal{O}(N)$ , while (ii)  $\sum_n |f_{i,k,n}| e^{j\vartheta_{i,k,n}}$  and  $n_k$  do not increase because the values of  $\vartheta_{i,k,n}, \forall n$  are different from each other. Hence, as  $N$  increases, we can determine the asymptotic SINR at UE  $k$  for ZFBF with the co-phasing approach as follows:

$$\gamma_k^{\text{full}} = \frac{N^2 \rho_k \zeta_k |c_k|^2 (\sum_n |f_{k,k,n}|/N)^2}{K^2 \|\bar{\mathbf{t}}_k\|^2} \xrightarrow{\text{a.s.}} \frac{N^2 \rho_k \zeta_k |c_k|^2 \mathbb{E} [|f_{k,k,n}|]^2}{K^2 \|\bar{\mathbf{t}}_k\|^2}. \tag{17}$$

In (17),  $\mathbb{E} [|f_{k,k,n}|]$  represents the expectation of the random variable  $|f_{k,k,n}|$  for  $n$ , where  $n$  ranges from 1 to  $N$ . From (17), it can be observed that, as  $N$  increases, the received SINR increases with  $\mathcal{O}(N^2)$ , and this is equivalent to the asymptotic SNR of an ideal RIS-assisted cellular network, as demonstrated in [22]. While the implementation of the ZFBF and the co-phasing technique may not be optimal, they have the potential to achieve optimal performance in the asymptotic regime. However, a general ZFBF requires complete CSI of  $\mathbf{h}_{k,k}$ , and the co-phasing technique requires complete CSI of  $\mathbf{f}_{k,k}$ . Acquiring complete CSI at the ES leads to a considerable increase in signaling overhead and introduces significant latency due to extended round-trip delays, particularly in SatCom systems. Therefore, in the next section, we propose a deterministic ZFBF and co-phasing technique that utilizes partial CSI.

### 3.2. ZFBF and Co-Phasing Technique Using Partial CSI

Acquiring complete CSI at the ES results in substantial signaling overhead, leading to significant latency. Additionally, due to the fully passive nature of the RIS, the ES cannot accurately estimate RIS-related channels such as  $\mathbf{D}_k$  and  $\mathbf{f}_{k,k}$ . In this regard, we propose a deterministic ZFBF and co-phasing technique that utilizes partial CSI.

Based on (13) and (14), we can observe that  $\mathbf{h}_{k,k} \bar{\mathbf{t}}_i = 0, \forall i \neq k$ . Motivated by this observation, we propose a ZFBF vector as  $\mathbf{w}_k = \bar{\mathbf{t}}_k / (K \|\bar{\mathbf{t}}_k\|)$ , which can perfectly eliminate the IBI as follows:

$$\begin{aligned} & \sum_{i \neq k}^K \sqrt{\rho_i} \mathbf{h}_{k,k} \mathbf{w}_i x_i \\ &= \sum_{i \neq k}^K \sqrt{\rho_i \zeta_k} |c_k| \exp(j\psi_k) \sum_n |f_{k,k,n}| \frac{\mathbf{a}_k^T \bar{\mathbf{t}}_i}{K \|\bar{\mathbf{t}}_i\|} x_i = 0. \end{aligned}$$

To design the proposed ZFBF vector  $w_k = \bar{t}_k / (K\|\bar{t}_k\|)$ , the ES requires access to  $a_k$  for all  $k$ , which consists of the deterministic beam pattern coefficients. These coefficients are deterministic information and can be accurately estimated using location-aware channel estimation based on global navigation satellite systems (GNSSs) [18]. Also, to maximize the desired signal power using partial CSI, the phase shifts at the RIS can be designed such that the reflected  $N$  signals from  $N$  LoS paths are aligned in phase as follows:  $\theta_{k,n} = -\angle \tilde{f}_{k,k,n}^*$ ,  $\forall k, n$ . Similarly, in (16), as  $N$  increases, both the IRI and the noise become negligible compared to the desired signal as follows:

$$\begin{aligned}
 y_k &= \frac{\sqrt{\rho_k \bar{\zeta}_k} |c_k| e^{j\psi_k} \sum_n (\bar{\beta}_{k,k} + \tilde{\beta}_{k,k} \tilde{f}_{k,k,n}^* e^{-j\angle \tilde{f}_{k,k,n}^*})}{K\|\bar{t}_k\|} x_k \\
 &+ \sum_{i \neq k}^K \frac{\sqrt{\rho_i \bar{\zeta}_i} |c_i| e^{j\psi_i} \sum_n |f_{i,k,n}| e^{j\tilde{\theta}_{i,k,n}}}{K\|\bar{t}_i\|} x_i + n_k \\
 &\stackrel{\text{a.s.}}{\rightarrow} \frac{N\sqrt{\rho_k \bar{\zeta}_k} |c_k| e^{j\psi_k} (\bar{\beta}_{k,k} + \tilde{\beta}_{k,k} E[\tilde{f}_{k,k,n}^* e^{-j\angle \tilde{f}_{k,k,n}^*}])}{K\|\bar{t}_k\|} x_k \\
 &\stackrel{(b)}{=} \frac{N\sqrt{\rho_k \bar{\zeta}_k} |c_k| e^{j\psi_k} \bar{\beta}_{k,k}}{K\|\bar{t}_k\|} x_k,
 \end{aligned} \tag{18}$$

where  $\tilde{f}_{k,k,n}$  is the  $n$ th element of  $\tilde{f}_{k,k}$  and  $\tilde{\theta}_{i,k,n} = \angle f_{i,k,n}^* - \angle \tilde{f}_{k,k,n}^*$ . In (18), (b) arises from the fact that  $E[\tilde{f}_{k,k,n}^* e^{-j\angle \tilde{f}_{k,k,n}^*}] = E[\tilde{f}_{k,k,n}^*] \cdot E[e^{-j\angle \tilde{f}_{k,k,n}^*}] = 0$ . Thus, to design the proposed RIS phase shift matrix, the ES only requires  $\tilde{f}_{k,k}$ , which consists of the deterministic LoS components, which can also be accurately estimated using location-aware channel estimation based on GNSSs. Using the proposed deterministic ZFBF and co-phasing technique, we can obtain the asymptotic SINR at UE  $k$  as follows:

$$\gamma_k^{\text{part}} = \frac{N^2 \rho_k \bar{\zeta}_k |c_k|^2 \bar{\beta}_{k,k}^2}{K^2 \|\bar{t}_k\|^2}. \tag{19}$$

From (19), we can observe that as  $N$  increases, the received SINR also increases with  $\mathcal{O}(N^2)$ , as seen in the case of the ZFBF with co-phasing approach using full CSI. Furthermore, in practical A2G channel models, the average and maximum values of the Rician factor measured in [23] are 10 dB and 20 dB, respectively. As a result,  $E[|f_{k,k,n}|]$  is approximately similar to  $\bar{\beta}_{k,k} |\exp(-j2\pi d_{k,k,n}/\lambda)| = \bar{\beta}_{k,k}$ , leading to  $\gamma_k^{\text{part}} \approx \gamma_k^{\text{full}}$ . In summary, the proposed beamforming scheme comprises two stages. First, to perfectly eliminate the IBI, the ZFBF vector is designed as follows:  $w_k = \bar{t}_k / (K\|\bar{t}_k\|)$ . Next, to maximize the designed signal power based on the partial CSI, the phase shifting of the RIS is designed as follows:  $\theta_{k,n} = -\angle \tilde{f}_{k,k,n}^*$ ,  $\forall k, n$ .

### 3.3. Asymptotic Performance Analysis

Next, we conduct an asymptotic analysis of the mean of the capacity (i.e., ergodic capacity) for the proposed deterministic beamforming. From (19), the ergodic capacity can be derived asymptotically for a large  $N$  as follows:

$$\begin{aligned}
 \mu_{R_k} &= E \left[ \log_2 \left( 1 + \frac{N^2 \rho_k \bar{\zeta}_k |c_k|^2 \bar{\beta}_{k,k}^2}{K^2 \|\bar{t}_k\|^2} \right) \right] \\
 &\approx \log_2 \left( \frac{N^2 \rho_k \bar{\zeta}_k \bar{\beta}_{k,k}^2}{K^2 \|\bar{t}_k\|^2} \right) + 2E[\log_2 |c_k|] \\
 &\stackrel{(c)}{=} \log_2 \left( \frac{N^2 \rho_k \bar{\zeta}_k \bar{\beta}_{k,k}^2}{K^2 \|\bar{t}_k\|^2} \right) - \frac{\log_2 10}{10} e^{\mu_k + \frac{\sigma_k^2}{2}},
 \end{aligned} \tag{20}$$

where  $\mu_k = \eta_k - \log(\log 10) + \log 20$  [18]. In (20), (c) arises from the characteristic of the double-log-normal distribution of  $|c_k| \sim \mathcal{L}^2\mathcal{N}(\eta_k, \sigma_k^2)$  and a large  $N$ . Similarly, the variance of  $R_k$  can be obtained by the following:

$$\begin{aligned} \sigma_{R_k}^2 &= \text{Var} \left[ \log_2 \left( 1 + \frac{N^2 \rho_k \zeta_k |c_k|^2 \bar{\beta}_{k,k}^2}{K^2 \|\bar{\mathbf{t}}_k\|^2} \right) \right] \\ &\stackrel{(d)}{\approx} 4\text{Var}[\log_2 |c_k|] \\ &= \left( \frac{\log_2 10}{10} \right)^2 (e^{\sigma_k^2} - 1) e^{2\mu_k + \sigma_k^2}, \end{aligned} \tag{21}$$

where (d) results from a large  $N$  approximation. Given that the values of  $\rho_k, \zeta_k, \bar{\beta}_{k,k}, \mu_k, \sigma_k$ , and  $\|\bar{\mathbf{t}}_k\|$  are deterministic, it is possible to obtain  $\mu_{R_k}$  and  $\sigma_{R_k}^2$  deterministically. Consequently, we can assess the performance of an RIS-assisted SatCom system in terms of ergodic capacity without the need for extensive simulations.

Based on the scaling law for  $N$ , we can observe from (20) that the ergodic capacity increases with  $\mathcal{O}(\log N)$ , while (21) shows that  $\sigma_{R_k}^2$  remains constant regardless of  $N$ . Therefore, we can characterize the outage probability, defined as the probability that  $R_k$  falls below a target value  $R_0$ , as follows:

$$P_o = \Pr(R_k < R_0) = \Pr(R_k - \mu_{R_k} < R_0 - \mu_{R_k}). \tag{22}$$

Consider a target value  $R_0 = \epsilon \cdot \mu_{R_k}$  where  $0 < \epsilon \leq 1$ . Then, we can obtain the outage probability as follows:

$$P_o = \Pr(R_k - \mu_{R_k} < (\epsilon - 1)\mu_{R_k}). \tag{23}$$

From (20), we can observe that

$$R_k - \mu_{R_k} \approx 2 \log_2 |c_k| + \frac{\log_2 10}{10} e^{\mu_k + \frac{\sigma_k^2}{2}}, \tag{24}$$

and thus, a random variable  $R_k - \mu_{R_k}$  is unrelated to  $N$ . Then, the probability density function (PDF) of the random variable  $R_k - \mu_{R_k}$  is not affected by the increase in  $N$ , while  $\mu_{R_k}$  increases with  $\mathcal{O}(\log N)$ . Hence, as  $N$  increases, the PDF of  $R_k - \mu_{R_k}$  remains unchanged, and  $(\epsilon - 1)\mu_{R_k}$  decreases, resulting in a decreasing  $P_o$ . Hence, with the increase in  $N$ , the outage probability decreases, thereby verifying the ability of an RIS to offer reliable SatCom services for a large  $N$  regime.

#### 4. Simulation Results and Analysis

We conduct extensive simulations to evaluate the performance of a practical RIS-assisted SatCom system, considering a limited number of reflecting elements  $N$ . It is assumed that a low equatorial orbit (LEO) satellite serves a cluster of 7 UEs through 7 RISs (i.e.,  $K = 7$ ). The noise power at each UE is given by  $\kappa_B T B$ , where  $\kappa_B, T$ , and  $B$  are the Boltzmann constant, noise temperature at each UE, and bandwidth per beam, respectively. To ensure statistical reliability, all simulations are averaged over a large number of independent runs, and the simulation parameters used are provided in Table 1 based on [17].

**Table 1.** Simulation parameters.

| Parameter                                      | Value              |
|--|--------------------|
| Orbit  | LEO (3.6 × 700 km) |
| Distance between UAV and UE                    | 1 km               |
| Carrier frequency                              | 2 GHz (L-band)     |
| $K, G_{\max}, \phi_{3\text{dB}}$               | 7, 49.5 dB, 3.2°   |
| Rician factor ( $\kappa_{i,k}, \forall i, k$ ) | 10 dB              |

Table 1. Cont.

| Parameter                                | Value                                     |
|--|---|
| UE antenna gain                          | 38.16 dB                                  |
| Transmit power                           | 50 dBW                                    |
| Boltzmann’s constant ( $\kappa_B$ )      | $1.38 \times 10^{-23}$ J/m                |
| Bandwidth per beam ( $B$ )               | 20 MHz                                    |
| Noise temperature ( $T$ )                | 300 K                                     |
| RIS element layout                       | 2D square lattice                         |
| RIS element spacing                      | 0.01 m                                    |
| Average rain attenuation ( $\forall k$ ) | 3 dB ( $\eta_k = -1.5617, \sigma_k = 1$ ) |

In Figure 2, the asymptotic ergodic capacity of the proposed scheme analyzed in (20) is verified. In this figure, “MRT without IBI and IRI” shows an ideal performance representing the case where the ES employs the maximum ratio transmission (MRT) to generate beamforming weights  $w_k = h_{k,k}^H / (K \|h_{k,k}\|)$  that align the transmitted signals towards the intended UE. On the other hand, “random phase shift” represents the scenario of random passive beamforming, where the phase shifts  $\theta_{k,n}, \forall k$ , and  $n$  are randomly determined. The figure demonstrates that the asymptotic ergodic capacity derived from (20) aligns well with the simulation results as the value of  $N$  increases. The proposed deterministic ZFBF combined with the co-phasing technique utilizes partial CSI but achieves a performance close to that obtained using full CSI. Moreover, when  $N = 64$ , the proposed deterministic beamforming achieves approximately 92.8% of the ideal performance, and it increases as  $N$  increases, further confirming the asymptotic optimality of the proposed scheme.

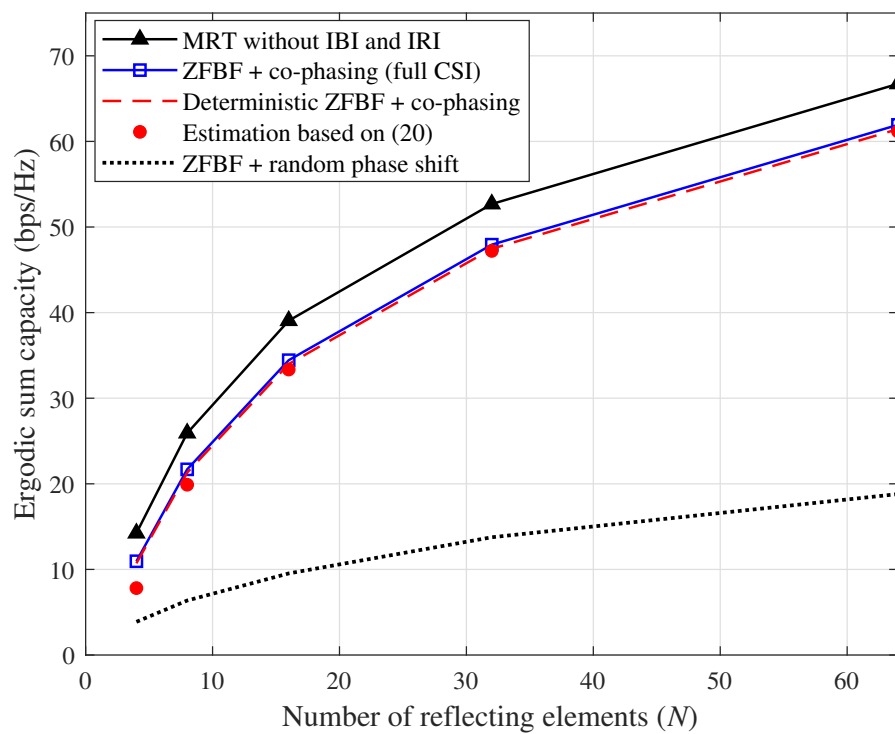


Figure 2. Performance comparison of the ergodic sum capacities for  $N$ .

In Figure 3, the outage probability analyzed in (23) is verified. The figure compares the outage probabilities obtained from the simulations for different values of  $\epsilon$ , specifically for  $\epsilon = 0.90, 0.85$ , and  $0.80$ . As shown in Figure 3, the outage probabilities tend to decrease

towards zero as  $N$  increases. This decreasing trend in the outage probability indicates improved system performance and enhanced reliability as the RIS is able to mitigate potential communication outages. Furthermore, Figure 3 demonstrates that the proposed deterministic ZFBF combined with the co-phasing technique utilizes partial CSI while achieving outage performance close to that obtained using full CSI. In conclusion, this result provides empirical evidence that supports the notion of the RIS as a viable solution for ensuring reliable SatCom in the presence of a large number of RIS elements.

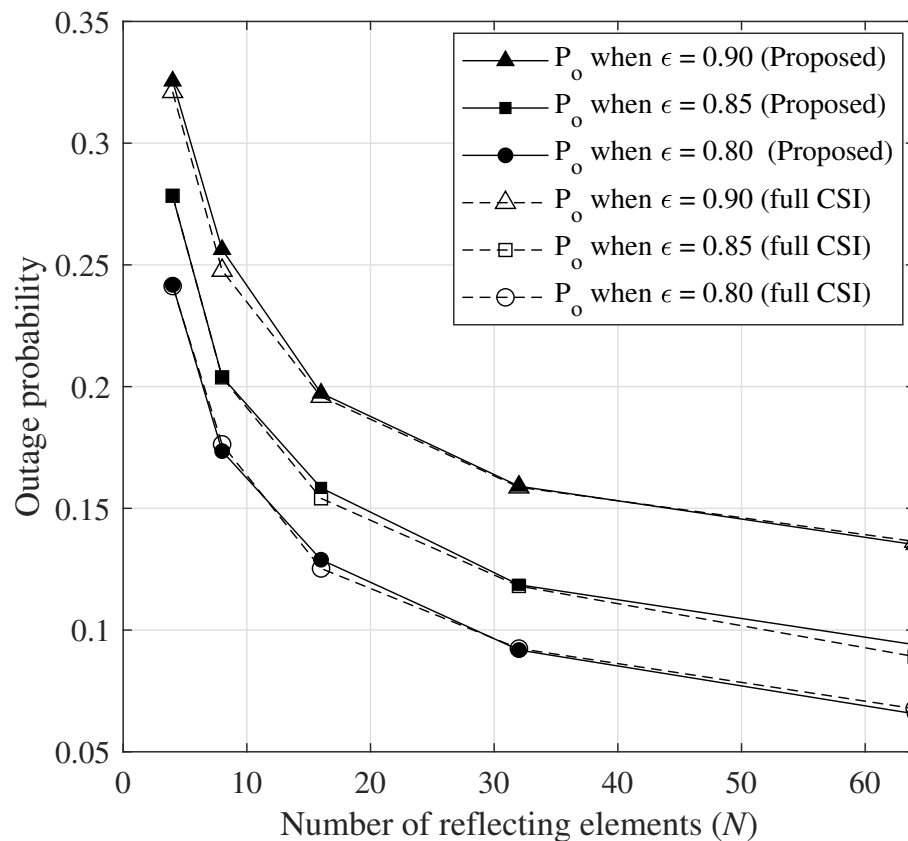


Figure 3. Performance comparison of the outage probabilities for  $N$ .

### 5. Conclusions

In this paper, we conducted an asymptotic analysis of a ZFBF combined with the co-phasing technique for mitigating IBI and IRI in RIS-assisted SatCom systems. In particular, we analyzed the performance of the ZFBF combined with co-phasing technique based on full CSI and demonstrated that IBI and IRI are asymptotically eliminated as the number of RIS elements increases to infinity. To make the analysis more practical, we proposed a novel deterministic ZFBF and co-phasing technique that only requires partial CSI, while still achieving asymptotic elimination of IBI and IRI. Furthermore, we derived a closed-form expression for the asymptotic ergodic capacity of the proposed scheme, allowing us to accurately determine the system’s performance without extensive simulations. Additionally, we proved that the outage probability decreases as  $N$  increases, confirming the RIS’s ability to provide reliable SatCom services in a large  $N$  regime. The simulation results validated the accuracy of our asymptotic analyses, and we observed consistent results between the approximated ergodic capacity and actual simulation results. Moreover, the proposed scheme demonstrated asymptotic optimality as it closely achieved the ideal performance, and this verifies the effectiveness of the proposed scheme in achieving optimal performance. Additionally, the outage probability demonstrated a potential convergence to zero as the number of RIS elements increases to infinity, further supporting the reliability and efficiency of the proposed scheme.

**Author Contributions:** Conceptualization, M.J.; methodology, T.K. and H.S.; software, M.J.; validation, M.J., T.K. and H.S.; formal analysis, M.J.; investigation, M.J.; resources, M.J.; data curation, M.J.; writing—original draft preparation, M.J.; writing—review and editing, T.K. and H.S.; visualization, M.J.; supervision, T.K. and H.S.; project administration, M.J., T.K. and H.S.; funding acquisition, M.J., T.K. and H.S. All authors have read and agreed to the published version of the manuscript.

**Funding:** This work was supported in part by Institute of Information & Communications Technology Planning & Evaluation (IITP) under the metaverse support program to nurture the best talents (IITP-2023-RS-2023-00254529) grant funded by the Korean government (MSIT) and by the National Research Foundation of Korea (NRF) grants funded by the Korean government (MSIT) (No. 2022R1F1A1064106, No. 2021R1C1C1012950, and No. 2021R1F1A1051075).

**Data Availability Statement:** Data are contained within the article.

**Conflicts of Interest:** The authors declare no conflicts of interest.

## References

1. Saad, W.; Bennis, M.; Chen, M. A Vision of 6G Wireless Systems: Applications, Trends, Technologies, and Open Research Problems. *IEEE Netw.* **2020**, *34*, 134–142. [\[CrossRef\]](#)
2. Wang, S.; Zhang, L.; Fan, H. An Enhanced Multi-Constraint Optimization Algorithm for Efficient Network Topology Generation. *Mathematics* **2023**, *11*, 3456. [\[CrossRef\]](#)
3. Xu, Y.; Deng, F.; Zhang, J. UDCO-SAGiMEC: Joint UAV Deployment and Computation Offloading for Space–Air–Ground Integrated Mobile Edge Computing. *Mathematics* **2023**, *11*, 4014. [\[CrossRef\]](#)
4. Son, H.; Jung, M. Phase Shift Design for RIS-Assisted Satellite-Aerial-Terrestrial Integrated Network. *IEEE Trans. Aerosp. Electron. Syst.* **2023**, *59*, 9799–9806; early access. [\[CrossRef\]](#)
5. Zhang, J.; Qi, C. Channel Estimation for mmWave Satellite Communications with Reconfigurable Intelligent Surface. In Proceedings of the 2021 IEEE Global Communications Conference (GLOBECOM), Madrid, Spain, 7–11 December 2021; pp. 1–6. [\[CrossRef\]](#)
6. Lin, Z.; Niu, H.; An, K.; Wang, Y.; Zheng, G.; Chatzinotas, S.; Hu, Y. Refracting RIS-Aided Hybrid Satellite-Terrestrial Relay Networks: Joint Beamforming Design and Optimization. *IEEE Trans. Aerosp. Electron. Syst.* **2022**, *58*, 3717–3724. [\[CrossRef\]](#)
7. Khan, W.U.; Lagunas, E.; Mahmood, A.; ElHalawany, B.M.; Chatzinotas, S.; Ottersten, B. When RIS Meets GEO Satellite Communications: A New Sustainable Optimization Framework in 6G. In Proceedings of the IEEE Vehicular Technology Conference, Helsinki, Finland, 19–22 June 2022; pp. 1–6. [\[CrossRef\]](#)
8. Rahman, M.H.; Sejan, M.A.S.; Aziz, M.A.; Kim, D.S.; You, Y.H.; Song, H.K. Deep Convolutional and Recurrent Neural-Network-Based Optimal Decoding for RIS-Assisted MIMO Communication. *Mathematics* **2023**, *11*, 3397. [\[CrossRef\]](#)
9. Rahman, M.H.; Sejan, M.A.S.; Aziz, M.A.; Kim, D.S.; You, Y.H.; Song, H.K. Spectral Efficiency Analysis for IRS-Assisted MISO Wireless Communication: A Metaverse Scenario Proposal. *Mathematics* **2023**, *11*, 3181. [\[CrossRef\]](#)
10. Yu, Y.; Wang, J.; Zhou, X.; Wang, C.; Bai, Z.; Ye, Z. Review on Channel Estimation for Reconfigurable Intelligent Surface Assisted Wireless Communication System. *Mathematics* **2023**, *11*, 3235. [\[CrossRef\]](#)
11. Singya, P.K.; Alouini, M.S. Performance of UAV-Assisted Multiuser Terrestrial-Satellite Communication System Over Mixed FSO/RF Channels. *IEEE Trans. Aerosp. Electron. Syst.* **2022**, *58*, 781–796. [\[CrossRef\]](#)
12. Zhao, J.; Gao, F.; Wu, Q.; Jin, S.; Wu, Y.; Jia, W. Beam Tracking for UAV Mounted SatCom on-the-Move With Massive Antenna Array. *IEEE J. Sel. Areas Commun.* **2018**, *36*, 363–375. [\[CrossRef\]](#)
13. Joo, C.; Choi, J. Low-delay broadband satellite communications with high-altitude unmanned aerial vehicles. *J. Commun. Netw.* **2018**, *20*, 102–108. [\[CrossRef\]](#)
14. Perez-Neira, A.I.; Vazquez, M.A.; Shankar, M.B.; Maleki, S.; Chatzinotas, S. Signal Processing for High-Throughput Satellites: Challenges in New Interference-Limited Scenarios. *IEEE Signal Process. Mag.* **2019**, *36*, 112–131. [\[CrossRef\]](#)
15. Hashida, H.; Kawamoto, Y.; Kato, N. Selective Reflection Control: Distributed IRS-Aided Communication With Partial Channel State Information. *IEEE Trans. Veh. Technol.* **2022**, *71*, 11949–11958. [\[CrossRef\]](#)
16. Al-Jarrah, M.; Al-Dweik, A.; Alsusa, E.; Iraqi, Y.; Alouini, M.S. On the Performance of IRS-Assisted Multi-Layer UAV Communications With Imperfect Phase Compensation. *IEEE Trans. Commun.* **2021**, *69*, 8551–8568. [\[CrossRef\]](#)
17. Kim, T.; Jung, M.; Son, H. Joint User Scheduling and Phase Shift Optimization for STAR-RIS-Assisted Multicast Satellite Communications. *IEEE Trans. Aerosp. Electron. Syst.* **2024**, 1–10. [\[CrossRef\]](#)
18. Ahmad, I.; Nguyen, K.D.; Letzepis, N.; Lechner, G.; Joroughi, V. Zero-Forcing Precoding With Partial CSI in Multibeam High Throughput Satellite Systems. *IEEE Trans. Veh. Technol.* **2021**, *70*, 1410–1420. [\[CrossRef\]](#)
19. Tse, D.; Viswanath, P. *Fundamentals of Wireless Communication*; Cambridge University Press: Cambridge, UK, 2005.
20. Basar, E.; Renzo, M.D.; de Rosny, J.; Debbah, M.; Alouini, M.S.; Zhang, R. Wireless Communications through Reconfigurable Intelligent Surfaces. *IEEE Access* **2019**, *7*, 116753–117773. [\[CrossRef\]](#)
21. Yu, W.; Cioffi, J. Constant-power waterfilling: Performance bound and low-complexity implementation. *IEEE Trans. Commun.* **2006**, *54*, 23–28. [\[CrossRef\]](#)

22. Wu, Q.; Zhang, R. Intelligent Reflecting Surface Enhanced Wireless Network via Joint Active and Passive Beamforming. *IEEE Trans. Wirel. Commun.* **2019**, *18*, 5394–5409. [[CrossRef](#)]
23. Cai, X.; Song, J.; Rodríguez-Piñeiro, J.; E. Mogensen, P.; Tufvesson, F. Characterizing the Small-Scale Fading for Low Altitude UAV Channels. In Proceedings of the International Conference on Wireless and Mobile Communications, Nice, France, 18–22 July 2021; pp. 16–19.

**Disclaimer/Publisher’s Note:** The statements, opinions and data contained in all publications are solely those of the individual author(s) and contributor(s) and not of MDPI and/or the editor(s). MDPI and/or the editor(s) disclaim responsibility for any injury to people or property resulting from any ideas, methods, instructions or products referred to in the content.